Research Article | Vol. 25, No. 13 | 26 Jun 2017 | OPTICS EXPRESS 14473
Optics EXPRESS

Autocorrelation z-scan technique for measuring the spatial and temporal distribution of femtosecond pulses in the focal region of lenses

P. CASTRO-MARÍN,[1] G. CASTRO-OLVERA,[1] J. GARDUÑO-MEJÍA,[1,*] M. ROSETE-AGUILAR,[1] N. C. BRUCE,[1] D. T. REID,[2] AND O. G. RODRÍGUEZ-HERRERA[1]

[1]*Centro de Ciencias Aplicadas y Desarrollo Tecnológico, Universidad Nacional Autónoma de México, Av. Universidad 3000, Coyoacán, Ciudad de México, 04510, Mexico*
[2]*Scottish Universities Physics Alliance (SUPA), Institute of Photonics and Quantum Sciences, School of Engineering and Physical Sciences, Heriot-Watt University, Riccarton, Edinburgh EH14 4AS, UK*
[*]*jesus.garduno@ccadet.unam.mx*

Abstract: In this work we present an Autocorrelation z-scan technique to measure, simultaneously, the spatial and temporal distribution of femtosecond pulses near the focal region of lenses. A second-order collinear autocorrelator is implemented before the lens under test to estimate the pulse width. Signals are obtained by translating a Two Photon Absorption (TPA) sensor along the optical axis and by measuring the second-order autocorrelation trace at each position z. The DC signal, which is typically not considered important, is taken into account since we have found that this signal provides relevant information. Experimental results are presented for different lenses and input wavefronts.

OCIS codes: (110.0110) Imaging systems; (320.0320) Ultrafast optics; (320.5550) Pulses; (320.7100) Ultrafast measurements.

References and links

1. W. Denk, J. H. Strickler, and W. W. Webb, "Two-photon laser scanning fluorescence microscopy," Science **248**(4951), 73–76 (1990).
2. S. B. Ippolito, B. B. Goldberg, and M. S. Unlu, "High spatial resolution subsurface microscopy," Appl. Phys. Lett. **78**(26), 4071–4073 (2001).
3. E. Ramsay, K. A. Serrels, M. J. Thomson, A. J. Waddie, M. R. Taghizadeh, R. J. Warburton, and D. T. Reid, "Three-dimensional nanoscale subsurface optical imaging of silicon circuits," Appl. Phys. Lett. **90**(13), 131101 (2007).
4. L. P. Ghislain, V. B. Elings, K. B. Crozier, S. R. Manalis, S. C. Minne, K. Wilder, G. S. Kino, and C. F. Quate, "Near-field photolithography with a solid immersion lens," Appl. Phys. Lett. **74**(4), 501–503 (1999).
5. K. A. Serrels, E. Ramsay, P. A. Dalgarno, B. D. Gerardot, J. A. O'Connor, R. H. Hadfield, R. J. Warburton, and D. T. Reid, "Solid immersion lens application for nanophotonic devices," J. Nanophotonics **2**(1), 021854 (2008).
6. M. Rutkauskas, D.T. Reid, J. Garduño-Mejía, M. Rosete-Aguilar, "Time-domain measurements reveal spatial aberrations in a sub-surface two-photon microscope," accepted for publication in Appl. Opt., (2017).
7. Y. Kim, P. Lu, T. D. Milster, and K. Kieu, "Hyper-numerical aperture (NA = 2.8) microscope using λ = 1.56 μm femtosecond source for multi-photon imaging," Biomed. Opt. Express **4**(10), 1786–1794 (2013).
8. M. Kempe and W. Rudolph, "Impact of chromatic and spherical aberration on the focusing of ultrashort light pulses by lenses," Opt. Lett. **18**(2), 137–139 (1993).
9. Zs. Bor and Z. L. Horváth, "Distortion of femtosecond pulses in lenses. Wave optical description," Opt. Commun. **94**(4), 249–258 (1992).
10. W. Amir, T. A. Planchon, C. G. Durfee, J. A. Squier, P. Gabolde, R. Trebino, and M. Müller, "Simultaneous visualization of spatial and chromatic aberrations by two-dimensional Fourier transform spectral interferometry," Opt. Lett. **31**(19), 2927–2929 (2006).
11. P. Castro-Marín, J. Garduño-Mejía, M. Rosete-Aguilar, N. C. Bruce, D. T. Reid, C. Farrell, and G. E. Sandoval-Romero, "Aberration analysis based on pinhole-z-scan method near the focal point of refractive systems," Proc. SPIE **9953**, 99530Q (2016).
12. P. Castro-Marín, G. Castro-Olvera, C. Ruíz, J. Garduño-Mejía, M. Rosete-Aguilar and N.C. Bruce, "Z-scan confocal method for indirect focus location," sent to Rev. Sci. Inst., (2017).

#288040 https://doi.org/10.1364/OE.25.014473
Journal © 2017 Received 3 Mar 2017; revised 16 May 2017; accepted 20 May 2017; published 16 Jun 2017

Optics EXPRESS

13. F. Träger, *Springer Handbook of Lasers and Optics* (Springer, 2012).
14. P. Castro-Marín, G. Kapellmann-Zafra, J. Garduño-Mejía, M. Rosete-Aguilar, and C. J. Román-Moreno, "Webcam autofocus mechanism used as a delay line for the characterization of femtosecond pulses," Rev. Sci. Instrum. **86**(8), 085114 (2015).
15. J. M. Dudley, D. T. Reid, W. Sibbett, L. P. Barry, B. Thomsen, and J. D. Harvey, "Commercial Semiconductor Devices for Two Photon Absorption Autocorrelation of Ultrashort Light Pulses," Appl. Opt. **37**(34), 8142 (1998).
16. A. Siegmann, *Lasers*. (University Science Books, 1986).
17. L. García-Martínez, M. Rosete-Aguilar, and J. Garduño-Mejia, "Gauss-Legendre quadrature method used to evaluate the spatio-temporal intensity of ultrashort pulses in the focal region of lenses," Appl. Opt. **51**(3), 306–315 (2012).
18. S. Anaya-Vera, L. García-Martínez, M. Rosete-Aguilar, N. C. Bruce, and J. Garduño-Mejia, "Temporal spreading generated by diffraction in the focusing of ultrashort light pulses with perfectly conducting spherical mirrors," J. Opt. Soc. Am. A **30**(8), 1620–1626 (2013).
19. O. G. Rodríguez-Herrera, M. Rosete-Aguilar, N. C. Bruce, and J. Garduño-Mejía, "Temporal widening of a short polarized pulse focused with a high numerical aperture aplanatic lens," J. Opt. Soc. Am. A **31**(4), 696–703 (2014).
20. N. C. Bruce, M. Rosete-Aguilar, O. G. Rodríguez-Herrera, J. Garduño-Mejía, and R. Ortega-Martínez, "Spatial chirp in the focusing of few-optical-cycle pulses by a mirror," J. Mod. Opt. **60**(13), 1037–1044 (2013).
21. F. C. Estrada-Silva, J. Garduño-Mejía, and M. Rosete-Aguilar, "Third-order dispersión effects generated by non-ideal achromatic doublets on sub-20 femtosecond pulses," J. Mod. Opt. **58**(10), 825–834 (2011).
22. M. A. González-Galicia, M. Rosete-Aguilar, J. Garduño-Mejía, N. C. Bruce, and R. Ortega-Martínez, "Effects of primary spherical aberration, coma, astigmatism and field curvature on the focusing of ultrashort pulses: homogenous illumination," J. Opt. Soc. Am. A **28**(10), 1979–1989 (2011).
23. P. Bowlan, P. Gabolde, and R. Trebino, "Directly measuring the spatio-temporal electric field of focusing ultrashort pulses," Opt. Express **15**(16), 10219–10230 (2007).

1. Introduction

Temporal compression and spatial aberration compensation of femtosecond pulses near to the Bandwidth Limited (BL) and Diffraction Limit at the focal plane of lenses is fundamental for applications where maximum peak intensity or resolution is necessary [1–7]. A fundamental part is the expanding and focusing system. BL-pulses propagating through a dispersive material suffer temporal spreading due to Group Velocity Dispersion (GVD) but they may also suffer a temporal spreading due to Propagation Time Delay (PTD) arising from the difference in arrival time between pulses propagating at different heights at the pupil of the focusing system [8,9]. The PTD is introduced by the chromatic aberration of the system. For a beam propagating parallel to the optical axis, spherical aberration also plays an important role in the spatial-temporal distribution of the focusing light [10]. In previous work [11,12] we presented two methods to study the spatial distribution of the light near the focal point of a refractive optical system. In these methods the relative focal position is measured by scanning a pinhole attached to the front of a power detector, along the optical axis, z, by using a motorized stage. A trace of Intensity vs. z is obtained by varying the pinhole position with the translation stage and recording the power meter reading as a function of the z position. We called these methods the Pinhole Masked Linear z-scan (PML z-scan) and the Z-scan confocal method for indirect focus location. Although some useful parameters for aberration analysis can be measured with the PML z-scan or with the z-scan confocal method, temporal measurements are not available.

In the present paper we introduce an Autocorrelation z-scan technique (AC-z-scan) to measure, simultaneously, the spatial and temporal distribution around the focal point. We describe the proposed AC-z-scan technique and the experimental setup. Finally experimental results for four lenses: an aspheric lens, an achromatic doublet and two apochromatic microscope objectives are presented. Results are also presented for two input wavefronts incident on the lens under test; an aberrated and a non-aberrated wavefront.

2. AC-z-scan technique

The AC-z-scan proposed in this paper consists of the implementation of a second-order collinear autocorrelator located before the lens under test to estimate the pulsewidth. Signals

Optics EXPRESS

are obtained by translating a Two Photon Absorption (TPA) sensor along the optical axis and by measuring the second-order autocorrelation trace at each position z around the focal point. In order to compress the pulse near to its BL at the TPA sensor, a GVD pre-compressor, based on a pair of prisms, is introduced. The main difference with respect to the PML z-scan method is the lack of a pinhole and the use of a photodiode instead of a power detector. In this case the intensity dependence, with respect to the z position, will be provided by the non-linear response of the TPA sensor itself. This procedure will provide the measurement of the function, $S_{Z-AC}(\tau,z)$ given by

$$S_{Z-AC}(\tau,z)=\int_{-\infty}^{\infty}\left|\left[E(t,z)+E(t-\tau,z)\right]^2\right|^2 dt \tag{1}$$

where τ is the time delay of the autocorrelation for each position z and $E(t,z)$ is the electric field. In this signal four main terms are present: a constant signal, the autocorrelation (intensity autocorrelation), the interferometric fringes, and its harmonics. The interferometric fringes and harmonic signal were filtered out to keep just two terms related to the individual TPA signals, from the two pulse replicas of the autocorrelator. The DC signal is typically not considered important; however, we have found that this signal provides relevant information. In Eq. (2) the DC terms and intensity autocorrelation are presented [13]:

$$\begin{aligned}S_{Z-AC}(\tau,z)=\int_{-\infty}^{\infty}\left[E^4(t,z)+E^4(t-\tau,z)+4E^2(t,z)E^2(t-\tau,z)\right]dt=\\ \int_{-\infty}^{\infty}\left[I^2(t,z)\right]dt+\int_{-\infty}^{\infty}\left[I^2(t-\tau,z)\right]dt+\int_{-\infty}^{\infty}\left[4I(t,z)I(t-\tau,z)\right]dt\end{aligned} \tag{2}$$

where $I(t,z)=\left|E(t,z)\right|^2$, which can be rewritten as:

$$S_{Z-AC}(\tau,z)=DC_{TPA}(z)+AC_{TPA}(\tau,z) \tag{3}$$

The AC-z-scan technique, based on the TPA measurement, can be separated in two terms: the $DC_{TPA}(z)$ generated by the first two terms in Eq. (2), in which the result of the integrals depend only on z, and the autocorrelation term $AC_{TPA}(\tau,z)$, the third term in Eq. (2) which depends on both, time delay and z. The DC signal can be extracted by using a low pass filter; a band pass filter is applied to extract the intensity autocorrelation, or by increasing the frequency of the delay line scan. The fringe filtering process can be performed by reducing the photodiode time response, for instance by coupling the photodiode to a high impedance device, or by increasing the frequency of the signal trace [14, 15]. In our case we changed the signal trace by speeding up the autocorrelator delay stage movement, until the fringes were washed out, for each step on the z-axis. With this we reduced the full acquisition time by a factor of 6, without compromising the detector sensitivity, and also filtering out most of the parasite signals.

Optics EXPRESS

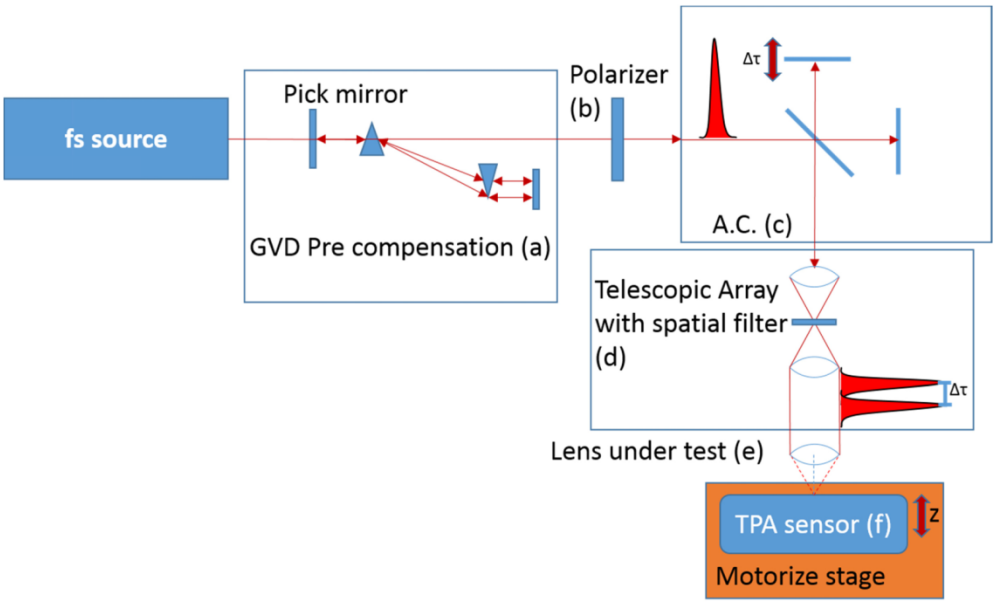

Fig. 1. Experimental set-up of the Autocorrelation z-scan technique (AC-z-scan).

3. Setup

The experimental setup, depicted in Fig. 1, uses a homemade femtosecond Ti:sapphire oscillator. This laser delivers an average power of 1.5W, near BL pulses of ~57fs@FWHM with a spectral bandwidth of about 17nm@800nm. The optical spectrum Fig. 2(a) and the intensity autocorrelation Fig. 2(b) of the output beam of the oscillator is presented.

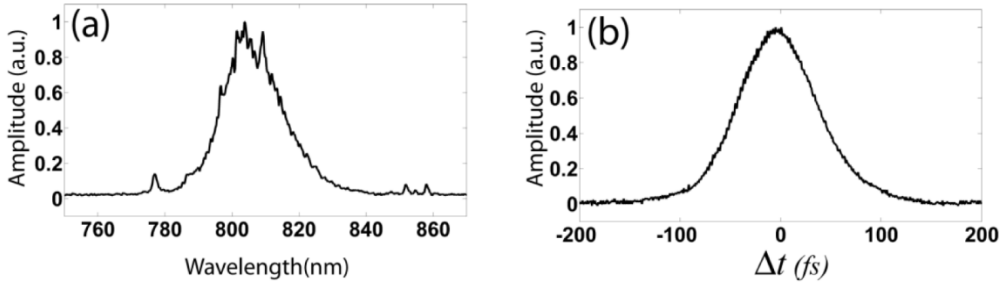

Fig. 2. (a) Optical spectrum and (b) Intensity Autocorrelation from the oscillator.

Optics EXPRESS

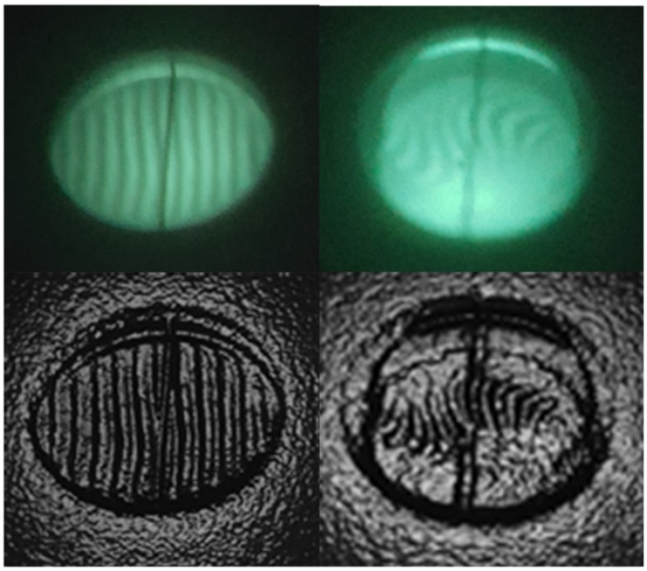

Fig. 3. (Top figures) Interference pattern snap shots of the collimated beam incident on the lens under test (with the laser working in CW mode operation) measured with a shear plate interferometer showing (a) a corrected wavefront and (b) an uncorrected wavefront. (Bottom figures) The same interference patterns but with a high pass filter.

A GVD pre-compensation stage was implemented, Fig. 1(a). The compressor was based on a pair of fused silica prisms (10SB10 Newport). For the input laser power control a polarizer MGTYE8 Karl-Lambercht was used, Fig. 1(b). The average input power for the experiment was 60mW to prevent saturation or damage in the TPA photodiode. The collinear autocorrelation measurements were performed with a Michelson interferometer with UFBS5050 Thorlabs beam splitter, Fig. 1(c), and a home-made delay line [14], with delay traveling distance of 390μm and a traveling time of 250ms. To expand the beam, a telescopic array including a spatial filter with a 20μm pinhole was placed, Fig. 1(d). The collimation and wavefront quality of the beam, incident on the lens under test, was confirmed with a shear plate interferometer. After the spatial filter the lens under test, Fig. 1(e), focuses the pulses at the TPA sensor (Hamamatsu G1115 GaAsP photodiode) with a 1MΩ resistance in parallel, mounted in a motorized translation stage (M-UTM50CC1DD Newport), with 1μm of resolution Fig. 1(f). Data collection was performed with a NI USB6211 DAQ with a sample rate of 10kS/s, and the whole experiment controlled with Labview. Two telescopic arrays were constructed to expand and collimate the beam, the first one was constructed with an aspheric lens, Thorlabs C220TME and an Edmund VIS-achromatic lens 25X160, giving the interference pattern presented in Fig. 3(a) and the second one with a microscope objective and a single lens, giving the interference pattern presented in Fig. 3(b). The interference patterns presented in Figs. 3(a) and 3(b) were obtained with a SI254 Thorlabs shear plate, placed after the telescopic array and before the lens under test, with the laser working in CW mode operation. It can be seen that the wavefront given by the first telescope array is corrected (see Fig. 3(a)) whereas the second array gives a highly-aberrated wavefront (see Fig. 3(b)). The data for the lenses under test are presented in Table 1.

Optics EXPRESS

Table 1. Parameters of the lenses under test.

Lens	Model	Focal length (mm)	Numerical Aperture (NA without iris)
Aspheric lens	Thorlabs, AL4532-B	32	0.61
Achromatic lens	NIR 12X40 Edmund 45-796	40	0.15
Apochromatic microscope objective 5X	Mitutoyo 378-822-5	40	0.14
Apochromatic microscope objective 10X	Mitutoyo 378-823-5	20	0.28

4. Experimental results

The data obtained, simultaneously, by this technique are presented in Fig. 4 for each lens under test using the telescopic array with corrected wavefront shown in Fig. 3(a). The $DC_{TPA}(z)$ vs. z results are represented by the blue line. These data sets include information about the intensity change along the z-axis and its distribution width along z, just as the information provided in the PML z-scan method with the iris. The z step used for the data set was 2μm, and the full data set acquisition time was 20 minutes. The larger the achieved maximum value of $DC_{TPA}(z)$ is, the larger the achieved peak intensity is. On the other hand, the narrower the width of this signal, $DC_{TPA}(z)$ vs. z (blue line), the shorter is the Rayleigh range. From reference [16], the Rayleigh range is defined as $z_R = \pi w_0^2/\lambda$, where w_0 is the beam waist and λ is the wavelength of the carrier. On the other hand, the effective diameter of a focused Gaussian spot by a lens is given by $d_0 \approx 2f\lambda/D$, where f is the focal length, D is the diameter of the lens and $d_0 = 2w_0$. Therefore the Rayleigh range can be expressed as:

$$z_R \approx \pi\lambda\left(\frac{f}{D}\right)^2 \tag{4}$$

The focal length for each lens is presented in Table 2 and the diameter of the beam incident on the lenses is $D = 8mm$ since an iris was placed in front of all lenses under test. We define the depth of field as $DOF = 2z_R$. The DOF calculated with Eq. (4) and the experimental DOF_{Exp} measured from the $DC_{TPA}(z)$ vs. z data sets, shown in Fig. 4, are presented in Table 2.

Table 2. Depth of field comparison. The DOF calculated with Eq. (4) and the DOF_{Exp} measured from the experiment $DC_{TPA}(z)$ vs. z @ $FWHM$ in Fig. 4.

	Aspheric	Achromatic	Apochromatic 5x	Apochromatic 10x
$DOF\ [mm]$	**0.08**	**0.12**	**0.12**	**0.03**
$DOF_{Exp}\ [mm]$	**0.08**	**0.11**	**0.11**	**0.04**

Optics EXPRESS

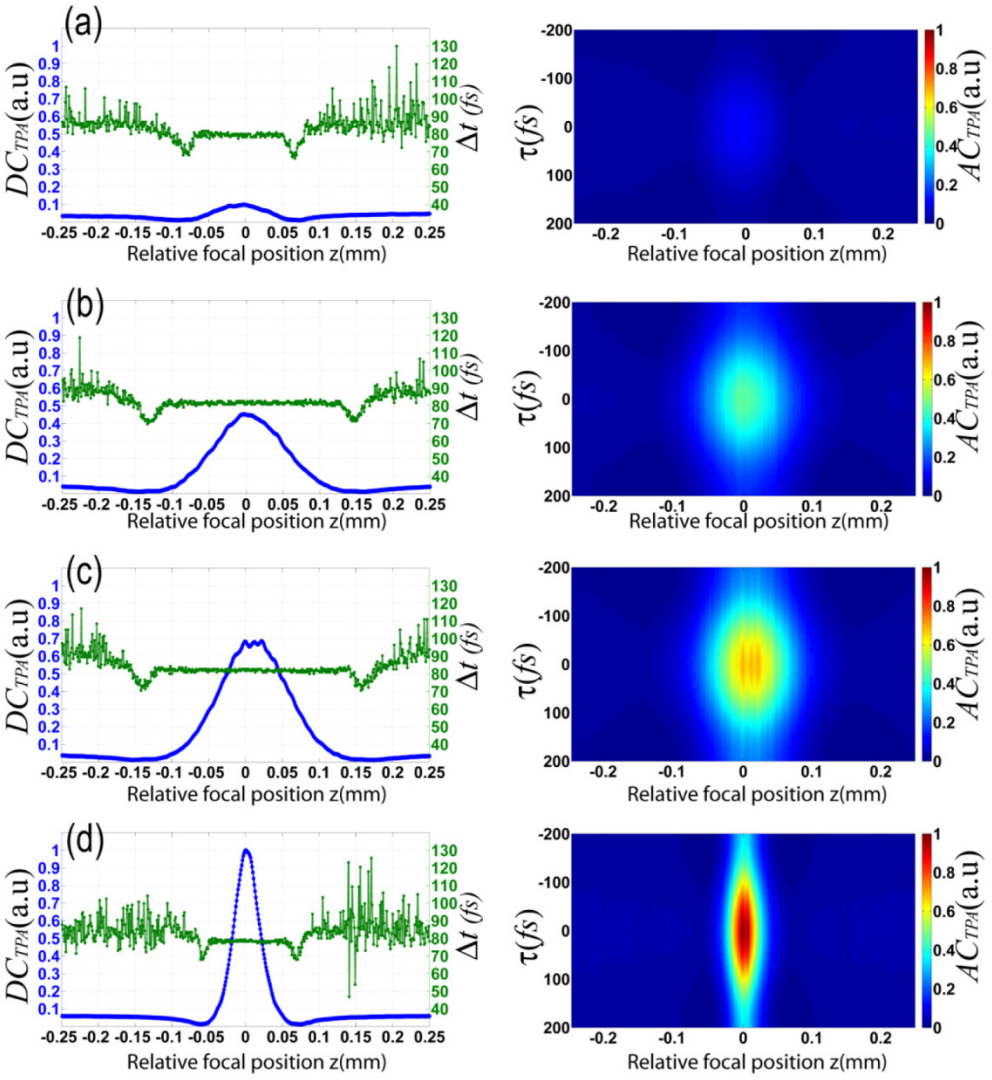

Fig. 4. Corrected wavefront. (Left column) the $DC_{TPA}(z)$ vs. z (blue line) and $\Delta t(z)$ vs. z (green line). (Right column) $AC_{TPA}(\tau, z)$ vs. z vs. time, (a) AL4532-B (Aspheric f = 32mm), (b) 45-796 (achromatic doublet f = 40 mm), (c) 378-822-5 (Apochromatic 5x), (d)37-823-5 (Apochromatic 10x). An iris open to 8mm was placed in front of the lenses.

From the results in Table 2, we can confirm that the $DC_{TPA}(z)$ vs. z signal provides information about the transversal intensity variation along the optical axis when the incident wavefront is aberration-free. The corresponding autocorrelation width, $\Delta t(z)$, green line, is extracted from the trace $AC_{TPA}(\tau, z)$ (right column in Fig. 4) for each slice of z. Autocorrelation width, $\Delta t(z)$, has been measured assuming a Gaussian pulse shape @ FWHM. According to these results, no change of pulsewidth around the focal point is observed in each case. This is due to the relatively narrow bandwidth of our *fs* source. According to theory, however, changes in pulse duration along z are expected for shorter pulses, below 10fs @ 800 nm [17–20]. For intensity normalization purposes, the maximum

Optics EXPRESS

value of the $DC_{TPA}(z)$ obtained among all lenses under test was used. With this, the results can be easily compared under the same input parameters (optical power 60mW and ~80fs). In each case, the pre-compressor was adjusted in order to compensate the GVD, introduced for each particular lens under test. In Fig. 4, for both $DC_{TPA}(z)$ vs. z (blue line) and $\Delta t(z)$ vs. z (green line), we can see that around the focal point, the intensity and pulse-width signal have dropped to a minimum value and then the signals start to rise again. This is related to a low optical photon flux where the thermal noise of the shunt resistance (of the semiconductor) and/or the photodiode leakage current noise becomes dominant [13]. The RMS error associated with the pulsewidth measurement $\Delta t(z)$ vs. z is approximately 0.6 fs.

We have also tested our method by introducing an aberrated-wavefront, (see Fig. 3(b)). Based on the symmetry of the traces and maximum intensity (see Fig. 5), it is possible to compare the correction capabilities of the apochromatic objectives with respect to the achromatic doublet and the aspherical lens.

From the experimental results presented in Figs. 4 and 5 we can conclude the following:

1. The optics used for expanding and focusing the beam introduces no propagation time delay (PTD) for pulses of 57fs (FWHM)@800nm.
2. It was possible to compress the pulses at the focal position near to the bandwidth limit. In other words, GVD and its variation across the aperture are well-compensated by the prism-compressor.
3. No change in temporal duration of the pulse was measured when the TPA-sensor was moved along the optical axis, z-axis. So in the absence of GVD and PTD, defocusing introduces no temporal spreading in the focused pulse.
4. For an aberration-free wavefront incident on the focusing lens under test, the Rayleigh range measured using the $DC_{TPA}(z)$ agrees with the theoretical Rayleigh range for a lens (see Table 2) otherwise it does not agree. This might be useful for testing the quality of the input wavefront on the focusing lens; especially when working with carrier wavelengths that are not in the visible range when it is difficult to see the interference pattern to test the quality of the wavefront.
5. In the absence of GVD and PTD, a highly-aberrated wavefront incident on the lens under test does not introduce temporal spreading in the focusing pulse. This result verifies other published work [21,22].
6. The peak of the $DC_{TPA}(z)$ signal gives the position for optimum coupling between space and time. The peak of the $DC_{TPA}(z)$ signal will be coincident with the position for best spatial resolution since there is no variation in pulse duration along-z-axis as shown in the trace $AC_{TPA}(\tau, z)$ vs. z in Figs. 4 and 5. In other words, the position for best spatial resolution can be located by the peak of the $DC_{TPA}(z)$ signal vs. z plot.

Optics EXPRESS

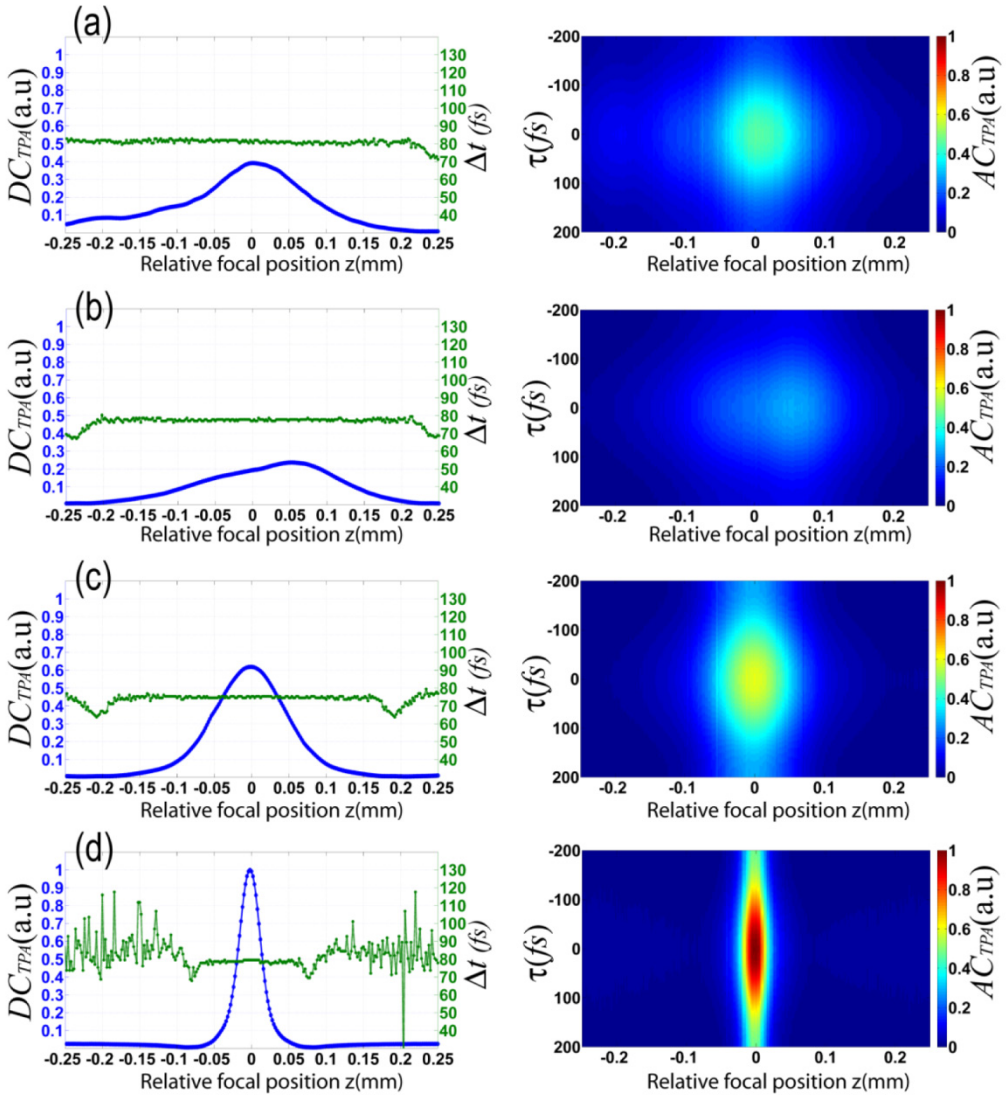

Fig. 5. Aberrated wavefront. (left column) the $DC_{TPA}(z)$ vs. z (blue line) and $t(z)$ vs. z (green line), (right column) $AC_{TPA}(\tau, z)$ vs. z vs. time, (a) AL4532-B (Aspheric f = 32mm), (b) 45-796 (achromatic doublet f = 40 mm), (c)378-822-5 (Apochromatic 5x), (d)37-823-5 (Apochromatic 10x)

It is important to mention that the normalization for the DC signal in Figs. 4 and 5 are with respect to the maximum intensity in each figure (given by lens 37-823), i.e., the normalization factor is not the same for Fig. 4 and Fig. 5. The maximum intensity for lens 37-823 in Fig. 4 is not the same as the maximum intensity for the same lens in Fig. 5, so the intensity distribution for the aspheric lens in Fig. 4.a cannot be compared directly to the intensity distribution for the same lens in Fig. 5a. The same is true for the other lenses.

Although the method provides no information of the variations along the transversal axes, in comparison with other work [23], it is very sensitive and simple to implement since it is based on a single TPA photodiode [15], with the possibility of extraction of additional information of the phase if the interferometric fringes are preserved during the acquisition.

Optics EXPRESS

5. Conclusions

In this work we have presented what we have called the Autocorrelation z-scan technique (AC-z-scan) to measure, simultaneously, spatial and temporal distributions of focused femtosecond pulses by using the DC signal, which is typically not considered important. We have found that this signal provides information on the transversal intensity variation along the optical axis. The signals were obtained by translating a Two Photon Absorption (TPA) sensor along the focal axis and by measuring the second-order autocorrelation trace at each position z around the focal point as well as the individual TPA contribution of the two pulse replicas of the autocorrelator. We have demonstrated the feasibility of this technique to evaluate the performance of different optical systems to focus femtosecond pulses with an aberrated and a non-aberrated input wavefront, allowing a full data set acquisition time of 20 minutes with a z-step of $2\mu m$ in a z-range of 0.5mm.

Funding

Dirección General de Asuntos del Personal Académico, Universidad Nacional Autónoma de México (DGAPA, UNAM) (PAPIIT-IG100615).

Acknowledgments

Pablo Castro-Marín and Gustavo Castro-Olvera acknowledge grants from Consejo Nacional de Ciencia y Tecnología (CONACyT), México and from the Programa de Maestría y Doctorado en Ingeniería, UNAM.